Nano Research
2019, 12(1): 115–119

ISSN 1998-0124 CN 11-5974/O4
https://doi.org/10.1007/s12274-018-2188-4

Research Article

Strong dual-crosslinked hydrogels for ultrasound-triggered drug delivery

Wenxu Sun[1,§], Heting Jiang[1,§], Xin Wu[1,§], Zhengyu Xu[1], Chen Yao[2,3], Juan Wang[1], Meng Qin[1], Qing Jiang[2,3], Wei Wang[1] (✉), Dongquan Shi[2,3] (✉), and Yi Cao[1] (✉)

[1] *Collaborative Innovation Center of Advanced Microstructures, National Laboratory of Solid State Microstructure, and Department of Physics, Nanjing University, Nanjing 210093, China*
[2] *Department of Sports Medicine and Adult Reconstructive surgery, Drum Tower Hospital; Medical School, State Key Laboratory of Analytical Chemistry for Life Science, Nanjing University, Nanjing 210008, China*
[3] *Joint Research Center for Bone and Joint Disease, Model Animal Research Center (MARC), School of Chemistry and Chemical Engineering, and State Key Laboratory of Analytical Chemistry for Life Science, Nanjing University, Nanjing 210093, China*
§ *Wenxu Sun, Heting Jiang, and Xin Wu contributed equally to this work.*

Received: 1 August 2018 / **Revised:** 18 August 2018 / **Accepted:** 23 August 2018

ABSTRACT

Hydrogels that can respond to dynamic forces either from endogenous biological activities or from external mechanical stimuli show great promise as novel drug delivery systems (DDS). However, it remains challenging to engineer hydrogels that specifically respond to externally applied mechanical forces with minimal basal drug leakage under normal stressful physiological conditions. Here we present an ultrasound responsive hydrogel-based DDS with special dual-crosslinked nanoscale network architecture. The covalent crosslinks endow the hydrogel high mechanical stability and greatly suppress deformation-triggered drug release. Meanwhile, the dynamic covalent boronate ester linkages between hydrogel backbone and the anti-inflammation compound, tannic acid (TA), allow effective ultrasound-triggered pulsatile release of TA. As such, the hydrogel shows distinct drug release profiles under compression and ultrasound. A proof-of-principle demonstration of the suppression of inflammation activation of macrophage upon ultrasound-triggered release of TA was also illustrated. We anticipate that this novel hydrogel-based drug delivery system can be used for the treatment of inflammatory diseases on load-bearing tissues, such as muscle and cartilage.

KEYWORDS

hydrogel, dynamic covalent bond, mechanical force, drug release

1 Introduction

Owing to their high biocompatibility and environmental responsiveness [1], hydrogels and microgels have been extensively explored for a variety of biological applications, including tissue engineering [2–4], wound dressing [5, 6], bioactuators [7–9] and drug delivery [10–12]. Many of these applications require the hydrogels to have considerable mechanical stability, as they are inevitably subjected to mechanical forces when functioning *in vivo* [13]. Forces generated in many physiological processes, such as muscle contraction [14], cartilage compression [15] and blood flow in the cardiovascular systems [16], can cause deformation and even disintegration of hydrogels. Forces are also involved in many pathological conditions, such as scar formation and inflammation [17]. Taking advantage of these special mechanical forces, hydrogels have been tailored as "smart" drug delivery systems (DDS) that can release encapsulated drugs upon mechanical stimuli [18–23]. These systems are promising for the treatment of some diseases [13, 24–26]. Parallel to the design of hydrogels responsive to internal mechanical forces, hydrogels that can control drug release upon various external mechanical stimuli, such as magnetic forces and ultrasound, have also been extensively explored [27–32]. These systems allow spatial, temporal and on-demand control of drug release [33–35]. However, it is not possible to distinguish intrinsic and external mechanical forces in biological settings. Many drug carriers that are designed to respond to external mechanical stimuli may also show considerable drug release induced by unavoidable endogenous mechanical forces. It remains a major challenge to engineer hydrogels that do not show significant basal drug release yet can still respond to external mechanical triggers.

Most mechanical force-responsive hydrogel-based drug delivery systems rely on the force induced dynamic or permanent changes of the hydrogel network to release encapsulated drugs [1, 30, 33]. Therefore, the hydrogels are designed to be mechanically weak so that they are sensitive to mechanical stimuli. In order to increase the mechanical stability of the hydrogels without jeopardizing the mechanical responsiveness, we decided to engineer a dual crosslinked (DC) hydrogel [36] with unique nanoscale network topology. In the DC gel, the permanent crosslinkers provide substantial mechanical stability to minimize the drug leakage under intrinsic mechanical stress and the dynamic crosslinkers can still effectively respond to external ultrasound stimuli. Moreover, the model drugs are linked to the hydrogels via dynamic covalent bonds, which further reduces endogenous force-triggered release. This novel hydrogel can be reliably used under substantial mechanical load and can respond to external mechanical force for on-demand drug release. We anticipate that they can be used for the treatment of diseases on load-bearing tissues, such as muscle and cartilage.

Address correspondence to Wei Wang, wangwei@nju.edu.cn; Dongquan Shi, shidongquan1215@163.com; Yi Cao, caoyi@nju.edu.cn

2 Results and discussion

Figure 1 shows the design of the DC gel-based drug delivery system. We chose methacrylic hyaluronic acid (HA) mixed with four-armed polyethylene-glycol acrylate (4arm-PEG-Aclt) as the backbone of the hydrogel. The permanently crosslinked hydrogel network was constructed through free radical polymerization. And the dynamic crosslinking was achieved through the formation of boronate ester bonds between phenyl boronic acid and a polyphenol compound, tannic acid (TA, Fig. S1 in the Electronic Supplementary Material (ESM)) from green tea. TA and other green tea derived polyphenols have been proven to have antibacterial, antioxidant [37], and anti-inflammatory properties and have been used for the treatment of arthritis [38, 39]. We used TA as the model drug and the dynamic crosslinker of the hydrogel. Inspired by the dynamic nature of boronate ester bonds at neutral pH [40–44], we hypothesized that they might be mechanically labile under physiological conditions compared to typical covalent bonds. HA bearing both methacrylic and phenyl boronic groups was synthesized in two steps as illustrated in Fig. 1(a). First HA was coupled with 4-(aminomethyl) phynyl boronic acid boronic acid to yield PhB-HA. Then, PhB-HA was reacted with methacrylic anhydride to get PhB-mHA. The grafting ratios of methacrylic and phenyl boronic groups were determined to be about 20% and 10% with respect to the HA repeating unit, respectively (Fig. S2 in the ESM). The hydrogels were prepared by copolymerization of PhB-mHA with 4arm-PEG-Aclt (M_W: 20 kDa) to produce the pre-gel with only the permanent crosslinked network. Then, the pre-gel was immersed in the phosphate buffer saline (PBS, pH = 7.4) solution containing different concentrations of TA to produce the final dual-crosslinked hydrogel (DC-gel). The proposed hydrogel network architecture is shown in Fig. 1(b). The photographs of the pre-gel and the DC-gel are shown in Fig. 1(c). Clearly, the hydrogel changed from transparent to brownish-green when being immersed in TA solutions, suggesting the formation of boronate ester bonds. Moreover, the swelling ratio of the pre-gels in PBS was ~ 1.3 times of the DC-gels (Fig. 1(c) and Fig. S3 in the ESM). The DC-gel was more compressible than the pre-gel presumably due to the presence of dynamic crosslinkers to dissipate energy (Fig. 1(c)). The presence of dual crosslinkers in the DC-gel was further verified by the rheological test. For the pre-gel, both *G*' and *G*" are low and remain constant over a broad angular frequency range, which is characteristic for the permanent network of hydrogels (Fig. 1(d)). In contrast, *G*' and *G*" of the DC-gel are much higher and depend on angular frequency, suggesting the presence of dynamic crosslinkers (Fig. 1(d)). The presence of additional crosslinkers in the DC-gel was also evidenced from scanning electron microscopy (SEM) images of the lyophilized gel samples (Figs. 1(e) and 1(f)), as the pore size for the DC-gel is much smaller than the pre-gel. Note that, the pore size of the hydrogels was tunable from more than 10 μm to less than 1 μm by simply adjusting the amount of TA components in the hydrogel (Figs. 1(e) and 1(f)). Using different ratios of PhB, TA and 4armed-PEG, we could obtain hydrogels with varied nanoscale pore size, crosslinking density, and drug loading–all these factors are important for drug delivery.

Next, we carried out extensive mechanical tests of the DC-gels prepared in solutions containing different TA concentrations. Uniaxial compression test showed that the Young's modulus of the DC-gels was enhanced with the increase of TA contents, confirming the crucial role of the dynamic covalent boronate ester bonds to the overall mechanical strength. The break strength increased from ~ 12 kPa for the pre-gels without TA to ~ 72 kPa for the DC-gels after immersing in PBS containing 0.5 mg·mL^{-1} of TA (Fig. 2(a)). In addition, the toughness was also improved from ~ 3.0 kJ·m^{-3} to more than 13.0 kJ·m^{-3} at the optimal conditions (Fig. 2(b)). Moreover, the properties of energy dissipation were also investigated systematically.

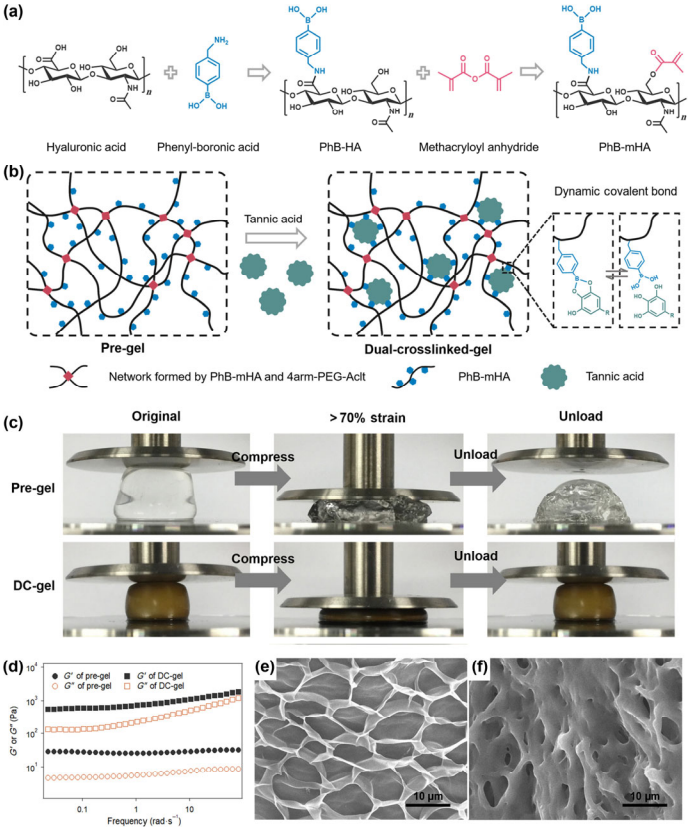

Figure 1 Schematic diagram of the dual-crosslinked hydrogel-based drug delivery system. (a) Synthetic process of phenyl-boronic-methacrylic-hyaluronic acid (PhB-mHA). (b) Schematic illustration of a modular DC-gel network composed of dynamic covalent interactions (blue polygon) and permanent covalent crosslinking (red diamond). (c) Optical image of the pre-gel (top) and the DC-gel (bottom) under different compressive conditions. (d) *G*' and *G*" values of the pre-gel and the DC-gel at different frequencies at room-temperature (1% strain). (e) SEM image of the pre-gel. (f) SEM image of the DC-gel. Scale bar: 10 μm.

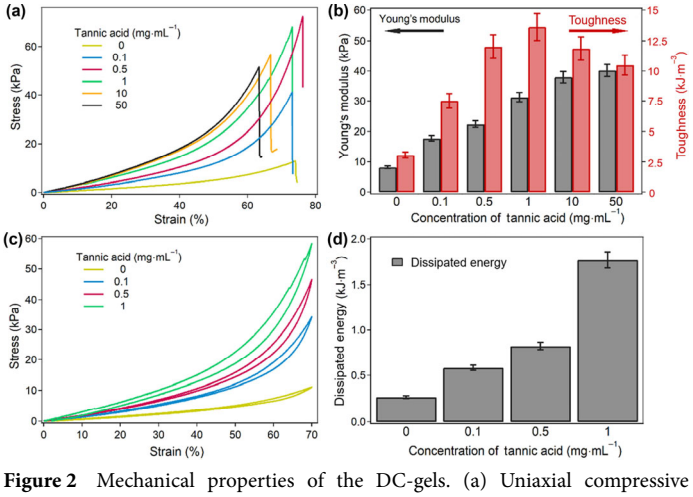

Figure 2 Mechanical properties of the DC-gels. (a) Uniaxial compressive stress-strain curve of different DC-gels. (b)Young's modulus and fracture energy for different DC-gels calculated from the uniaxial compressive stress-strain curves. (c) Uniaxial compression-relaxation cycles to a final strain of 70% for different DC-gels. (d) Dissipated energy for different DC-gels calculated from the uniaxial compression-relaxation cycles to a final strain of 70% curves.

Without TA, negligible hysteresis was shown between compression and relaxation traces indicating that there was no significant energy dissipation when only presence of permanent covalent network in the hydrogel (Fig. 2(c)). However, when TA was added to the system to establish the dynamic covalent cross-linking between boronic-acid and catechol, the hysteresis in the compression-relaxation cycles

was greatly increased. As shown in Fig. 2(d), with the increase of TA concentrations from 0 to 1 mg·mL^{-1}, the dissipated energy raised about seven times indicating the rupture of the dynamic covalent bonds by mechanical force. It is worth noting that mechanical force from the deformation of the hydrogel network cannot fully rupture all boronate ester bonds formed between TA and the polymer network. Once only a single boronate ester bond is remaining, force cannot transduce to the bond anymore (Fig. S4 in the ESM). Therefore, even the hydrogel was compressed to a strain of 60% for 10 h, no observable leakage of TA was observed (Fig. 3(a)). Nonetheless, these results confirmed great mechanical stability of the DC-gels and low basal leakage of drug under mechanical load, demonstrating its great potential to function in mechanically stressful environment for controlled drug release upon external mechanical stimuli.

Next, we tested whether ultrasound can be used as an external mechanical stimulus to trigger the release of TA from the DC-gels. Ultrasound provides solvodynamic shear force to the bonds between TA and the polymer network and in principle can release all boronate ester bonds. As shown in Fig. 3(a), the basal release of TA from the DC-gel was only ~ 2% over 10 hours. Such low spontaneous release rate can be attributed to the covalent link between drug and hydrogel network. The release rate is almost constant, which is distinct from typical diffusion-controlled release of non-covalently loaded drugs in the nano-network of hydrogel-based DDS. Based on this measurement, the drug cannot be fully released from the DC-gel in a period of a few months if no external mechanical force was applied. However, when treating with ultrasound every hour for 5, 10, and 20 min, we observed significantly enhanced release of TA (Fig. 3(b)). The longer the ultrasound time, the faster the release of TA. Moreover, TA typically showed a burst release immediately upon ultrasound treatment, suggesting that release of TA was originated from the dynamic breakage instead of permanent damage of the hydrogel network. These experiments suggested that the DC-gels can indeed be used for the treatment of chronic diseases, which requires long-term control of drug release.

Inflammation was associated with many chronic diseases, including rheumatic arthritis (RA), systemic lupus erythematosus (SLE), and progressive systemic sclerosis (PSS) [45]. To evaluate whether the release of TA from the DC-gels by ultrasound can indeed suppress inflammation, we developed a minimal *in vitro* system based on the mouse macrophage cell, RAW 264.7 (Fig. 4(a)). Ultrasound treatments and the presence of the DC-gels did not affect the viability of RAW 264.7 (Figs. S5 and S6 in the ESM). The initiation of inflammation response of RAW 264.7 was triggered by treating with 200 ng·mL^{-1} of lipopolysaccharide (LPS). The release of the cytokine, IL-6 and TNF-α directly indicated the inflammation activation of RAW 264.7 cells. The amount of TNF-α and IL-6 reached the peak value at the time point of 12 and 24 h after treatment, respectively (Fig. S7 in the ESM). For convenience, the concentration of TNF-α at the time point of 12 h was chosen as an indicator of the inflammation level. Then, the RAW 264.7 cells stimulated by LPS were treated by exposing to the DC-gels and applying 10 ultrasound cycles (the DC-gel group). For comparison, the cells without LPS treatment (the UT group), with LPS treatment but in the absence of any hydrogels (the LPS group), and with LPS treatment in the presence of the pre-gel (the pre-gel group) were also studied. Clearly, after the ultrasound triggered release of TA from the DC-gels, the concentration of TNF-α reduced to the same level as the UT group, suggesting the efficient suppression of inflammation response of macrophage cells (Fig. 4(b)). Note that, without ultrasound triggered release of TA, the DC-gel alone cannot reduce TNF-α secretion (Fig. 4(b)). These results clearly indicate the potential use of the DC-gels for the treatment of many chronic autoimmune diseases associated with uncontrolled inflammation.

3 Conclusion

In summary, we have designed a dual-crosslinked hydrogel with boronate ester bonds between tannic acid and phenyl boronic acid as the dynamic crosslinkers. Thanks to the novel hydrogel network structure, the hydrogels are mechanically strong and do not respond to mechanical forces transduced through the deformation of the hydrogel network. However, such hydrogels can still respond to external mechanical stimuli applied through ultrasound. The release of tannic acid can be triggered non-evasively and on-demand. The concept of using the dual-crosslinked hydrogels for decoupling endogenous mechanical force from physiological activity to external

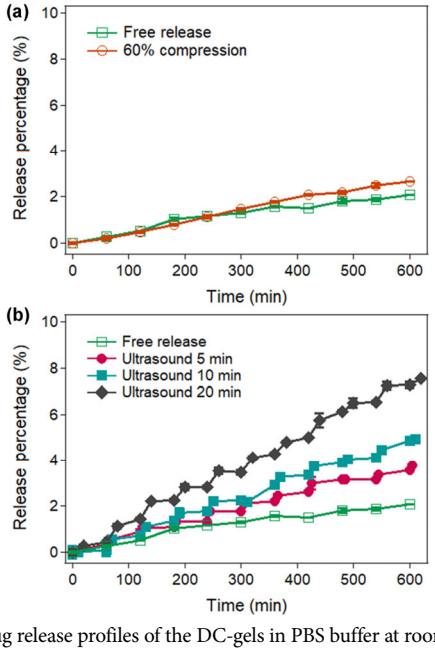

Figure 3 Drug release profiles of the DC-gels in PBS buffer at room temperature. (a) Profiles under constant compressive strain of 60% and zero strain (free release). (b) Profiles under ultrasound pulse of different time duration (0, 5, 10, and 20 min, respectively). Error bars correspond to S.E.M.

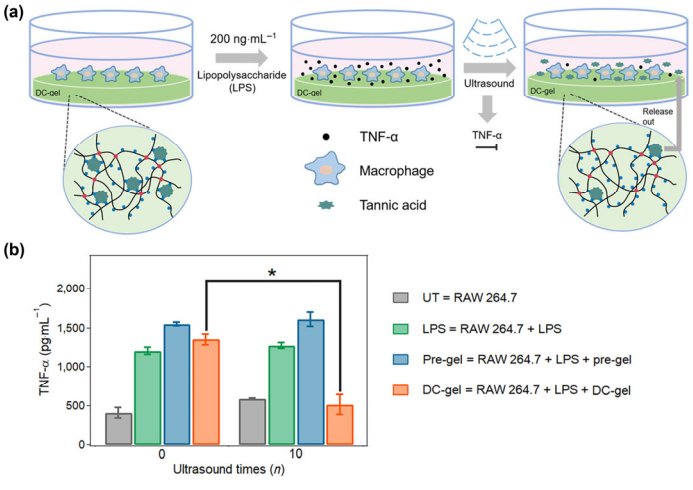

Figure 4 Tannic acid released from the DC-gels by ultrasound suppresses TNF-α secretion from RAW 264.7 cells with LPS stimulation. (a) Schematic diagram of the design of the *in vitro* experiments. (b) The amount of TNF-α released from mouse macrophage. The amount of TNF-α secretion from RAW 264.7 cells treated with 200 ng·mL^{-1} of LPS (green column) was up-regulated about 2.3 fold, compared to un-treated (UT) cells (gray column). The treatment of ten ultrasound cycles suppressed TNF-α secretion in stimulated RAW 264.7 cells in the presence of the DC-gels (orange column), while no change in the pre-gel group was observed (blue column).

mechanical signals represents an important step towards the clinic application of external mechanical force triggered drug delivery for complicated diseases. The proof-of-concept experiments show great potential of this system for the treatment of uncontrolled inflammation of many chronic autoimmune diseases.

4 Experimental

4.1 Mechanical measurements

The hydrogels were carefully transferred to the rheometer plate of the Thermo Scientific Haake Rheostress 6,000 and equilibrated for at least 10 min prior to the measurement. The rheology experiments were then carried out using a frequency-sweep mode with frequency of 1–100 rad·s^{-1} at 0.1% strain (geometry: 1°/20 mm of cone and plate; gap: 0.05 mm; temperature: 20 °C).

4.2 Scanning electron microscope

SEM images of the nanostructure of the hydrogels were taken using a Quanta Scanning Electron Microscope (Quata 200, FEI) at 20 kV. The hydrogels were lyophilized prior to the measurement.

4.3 Compressive test

The compressive stress-strain measurements were performed using a tensile-compressive tester (Instron-5944 with a 2 kN sensor) in the air. In compression-fracture test, the rate of compression was kept constant as 2% s^{-1} with respect to the original height of the hydrogel, roughly in a range of 8–12 mm·min^{-1}. In the compression-relaxation cycle test, the rate of compression was kept constant as 4% s^{-1} with respect to the original height of the hydrogel, roughly in a range of 16–24 mm·min^{-1}. The stress (σ) was calculated as the compression force divided by the cross-section area based on Eq. (1), in which F is the compression force, A_0 is the original cross-section area of the gels and ε is the strain. The E_f was calculated by the integration of the area below the compression stress-strain curves until fracture point according to the Eq. (2), in which ε_0 and ε_f correspond to the starting strain and the fracture strain of the compression, respectively. The dissipated energy (E_d) was a parameter used to characterize the capacity of hydrogels to dissipate energy and it was calculated by the integration of the area below the compression-relaxation cycles to a final strain of 70% for different DC-gels according to the Eq. (3), in which $\varepsilon_{0\%}$ and $\varepsilon_{70\%}$ correspond to the 0% strain and the 70% strain of the compression, respectively. In the Eq. (3), the $\sigma_c(\varepsilon)$ was the compression stress-strain curves and the $\sigma_r(\varepsilon)$ was the relaxation stress-strain curves. In addition, the compression Young's moduli were the approximate linear fitting values of the stress-strain curves in the strain range of ~ 5%–20%.

$$\sigma(\varepsilon) = \frac{F}{A_0}(1-\varepsilon) \tag{1}$$

$$E_f = \int_{\varepsilon_0}^{\varepsilon_f} \sigma(\varepsilon)\mathrm{d}\varepsilon \tag{2}$$

$$E_d = \int_{\varepsilon_{0\%}}^{\varepsilon_{70\%}} \sigma_c(\varepsilon)\mathrm{d}\varepsilon - \int_{\varepsilon_{0\%}}^{\varepsilon_{70\%}} \sigma_r(\varepsilon)\mathrm{d}\varepsilon \tag{3}$$

4.4 Drug release *in vitro* under different compressive strain

To qualitatively assess tannic acid release from the DC-gels, the DC-gels (approximately 0.8 mL per gel, n = 2) were immersed in PBS buffer (pH = 7.4, 20 mL) at room temperature. The gels were treated with different compressive strain (0% and 60%) and then the concentration of the tannic acid in the PBS was measured by UV-Vis (Nanodrop 2000 spectrophotometer, Thermo Scientific) at designated time intervals (1 h) for 10 h. The UV absorption values at 276 nm were used to quantify the releasing of tannic acid, and the concentrations(c_t) were calculated from the calibration curve (Fig. S8 in the ESM). The percentage of release ($p(t)$) at different time points was calculated from Eq. (4), in which the c_1, c_2, and c_3 were the parameters measured in the preparation process of the DC-gels.

$$p(t) = \frac{c_t}{c_1 - c_2 - c_3} \times \frac{2}{5} \times 100(\%) \tag{4}$$

4.5 Drug release *in vitro* after different ultrasound time

To qualitatively assess tannic acid release from the DC-gels, the DC-gels (approximately 0.8 mL per gel, n = 4) were immersed in PBS buffer (pH = 7.4, 20 mL) at room temperature. The gels were treated with a bench-top ultrasound (SHUMEI, KQ3200DV, 150W) for different time (0, 5, 10 and 20 min, respectively) and then the concentration of the tannic acid in the PBS was measured by a UV-Vis (Nanodrop 2000 spectrophotometer, Thermo Scientific) at designated time intervals (1 h) right before and after ultrasound treatment in a period of 10 h. The UV absorption values at 276 nm were used to calculate the concentrations(c_t) of the released tannic acid based on the calibration curve (Fig. S8 in the ESM). The release percentage of release ($p(t)$) at different time points was calculated from Eq. (4).

4.6 Cell culture and LPS treatment

Mouse macrophage cell line RAW 264.7, a gift from Prof. Yiqiao Hu, Nanjing University, was cultured in DMEM culture medium supplemented with with 10% FBS (Gibco, MA, USA), 100 U·mL^{-1} penicillin, and 100 μg·mL^{-1} streptomycin sulfate (Hyclone, USA). The cultivation was performed at 37 °C under a humidified atmosphere of 5% CO_2.

RAW 264.7 macrophage cells (2.5×10^4 cells per well in a 96-well plate) were incubated with or without 200 ng·mL^{-1} of LPS (Lipopolysaccharides from *Escherichia coli* O127:B8, Sigma, Germany). The supernatant in the cell cultivation wells was collected at different time points for subsequent cytokine analysis.

4.7 Cell viability and inflammatory tests

For the viability of cells at different time points of various treatments, the cell viability was determined by Cell Counting Kit-8, according to the manufacturer's instructions (Dojindo Laboratories, China).

The relative cell viability is calculated by Eq. (5).

Relative cell viability = [(mean cell viability determined in sample)/(mean cell viability determined in control)] × 100 (5)

Cell-free supernatants were collected at different time points and stored at −20 °C until determination. The concentrations of TNF-α, IL-6 and IL-1β in the supernatants of RAW 264.7 cell cultures were determined using an ELISA kit, according to the manufacturer's instructions (Beyotime, China).

4.8 Statistical analysis

Statistical significance was determined using one-way analysis of variance (ANOVA) followed by t test. Statistical significance was set to a P value < 0.05.

Acknowledgements

This research is supported mainly by the National Natural Science Foundation of China (Nos. 21522402, 11674153, 81622033 and 21774057) and the Fundamental Research Funds for the Central Universities (No. 020414380080).

Electronic Supplementary Material: Supplementary material is

available in the online version of this article at https://doi.org/10.1007/s12274-018-2188-4.

References

[1] Lu, Y.; Aimetti, A. A.; Langer, R.; Gu, Z. Bioresponsive materials. *Nat. Rev. Mater.* **2016**, *2*, 16075.

[2] Drury, J. L.; Mooney, D. J. Hydrogels for tissue engineering: Scaffold design variables and applications. *Biomaterials* **2003**, *24*, 4337–4351.

[3] Wang, H. Y.; Heilshorn, S. C. Adaptable hydrogel networks with reversible linkages for tissue engineering. *Adv. Mater.* **2015**, *27*, 3717–3736.

[4] Slaughter, B. V.; Khurshid, S. S.; Fisher, O. Z.; Khademhosseini, A.; Peppas, N. A. Hydrogels in regenerative medicine. *Adv. Mater.* **2009**, *21*, 3307–3329.

[5] Jayakumar, R.; Prabaharan, M.; Sudheesh Kumar, P. T.; Nair, S. V.; Tamura, H. Biomaterials based on chitin and chitosan in wound dressing applications. *Biotechnol. Adv.* **2011**, *29*, 322–337.

[6] Koehler, J.; Brandl, F. P.; Goepferich, A. M. Hydrogel wound dressings for bioactive treatment of acute and chronic wounds. *Eur. Polym. J.* **2018**, *100*, 1–11.

[7] Xue, B.; Qin, M.; Wang, T. K.; Wu, J. H.; Luo, D. J.; Jiang, Q.; Li, Y.; Cao, Y.; Wang, W. Electrically controllable actuators based on supramolecular peptide hydrogels. *Adv. Funct. Mater.* **2016**, *26*, 9053–9062.

[8] Pei, Z. Q.; Yang, Y.; Chen, Q. M.; Terentjev, E. M.; Wei, Y.; Ji, Y. Mouldable liquid-crystalline elastomer actuators with exchangeable covalent bonds. *Nat. Mater.* **2014**, *13*, 36–41.

[9] Fratzl, P.; Barth, F. G. Biomaterial systems for mechanosensing and actuation. *Nature* **2009**, *462*, 442–448.

[10] Li, J. Y.; Mooney, D. J. Designing hydrogels for controlled drug delivery. *Nat. Rev. Mater.* **2016**, *1*, 16071.

[11] Zhang, S. F.; Ermann, J.; Succi, M. D.; Zhou, A.; Hamilton, M. J.; Cao, B.; Korzenik, J. R.; Glickman, J. N.; Vemula, P. K.; Glimcher, L. H. et al. An inflammation-targeting hydrogel for local drug delivery in inflammatory bowel disease. *Sci. Transl. Med.* **2015**, *7*, 300ra128.

[12] Zhang, X. L.; Dong, C. M.; Huang, W. Y.; Wang, H. M.; Wang, L.; Ding, D.; Zhou, H.; Long, J. F.; Wang, T. L.; Yang, Z. M. Rational design of a photo-responsive UVR8-derived protein and a self-assembling peptide-protein conjugate for responsive hydrogel formation. *Nanoscale* **2015**, *7*, 16666–16670.

[13] Zhang, Y. Q.; Yu, J. C.; Bomba, H. N.; Zhu, Y.; Gu, Z. Mechanical force-triggered drug delivery. *Chem. Rev.* **2016**, *116*, 12536–12563.

[14] Sverdlova, N. S.; Witzel, U. Principles of determination and verification of muscle forces in the human musculoskeletal system: Muscle forces to minimise bending stress. *J. Biomech.* **2010**, *43*, 387–396.

[15] Mansour, J. M. Biomechanics of cartilage. In *Kinesiology*: *The Mechanics and Pathomechanics of Human Movement*; Oatis, C. A., Ed.; Wolter Kluwer: Philadelphia, 2003; pp 66–79.

[16] Zamir, M. Shear forces and blood vessel radii in the cardiovascular system. *J. Gen. Physiol.* **1977**, *69*, 449–461.

[17] Barnes, L. A.; Marshall, C. D.; Leavitt, T.; Hu, M. S.; Moore, A. L.; Gonzalez, J. G.; Longaker, M. T.; Gurtner, G. C. Mechanical forces in cutaneous wound healing: Emerging therapies to minimize scar formation. *Adv. Wound Care* **2018**, *7*, 47–56.

[18] Lee, K. Y.; Peters, M. C.; Anderson, K. W.; Mooney, D. J. Controlled growth factor release from synthetic extracellular matrices. *Nature* **2000**, *408*, 998–1000.

[19] Van Der Schaft, D. W. J.; Van Spreeuwel, A. C. C.; Van Assen, H. C.; Baaijens, F. P. T. Mechanoregulation of vascularization in aligned tissue-engineered muscle: A role for vascular endothelial growth factor. *Tissue Eng. Part A* **2011**, *17*, 2857–2865.

[20] Holme, M. N.; Fedotenko, I. A.; Abegg, D.; Althaus, J.; Babel, L.; Favarger, F.; Reiter, R.; Tanasescu, R.; Zaffalon, P. L.; Ziegler, A. et al. Shear-stress sensitive lenticular vesicles for targeted drug delivery. *Nat. Nanotechnol.* **2012**, *7*, 536–543.

[21] Korin, N.; Kanapathipillai, M.; Matthews, B. D.; Crescente, M.; Brill, A.; Mammoto, T.; Ghosh, K.; Jurek, S.; Bencherif, S. A.; Bhatta, D. et al. Shear-activated nanotherapeutics for drug targeting to obstructed blood vessels. *Science* **2012**, *337*, 738–742.

[22] Lu, Y.; Hu, Q. Y.; Lin, Y. L.; Pacardo, D. B.; Wang, C.; Sun, W. J.; Ligler, F. S.; Dickey, M. D.; Gu, Z. Transformable liquid-metal nanomedicine. *Nat. Commun.* **2015**, *6*, 10066.

[23] Di, J.; Yu, J. C.; Wang, Q.; Yao, S. S.; Suo, D. J.; Ye, Y. Q.; Pless, M.; Zhu, Y.; Jing, Y.; Gu, Z. Ultrasound-triggered noninvasive regulation of blood glucose levels using microgels integrated with insulin nanocapsules. *Nano Res.* **2017**, *10*, 1393–1402.

[24] Ye, Y. Q.; Wang, J. Q.; Hu, Q. Y.; Hochu, G. M.; Xin, H. L.; Wang, C.; Gu, Z. Synergistic transcutaneous immunotherapy enhances antitumor immune responses through delivery of checkpoint inhibitors. *ACS Nano* **2016**, *10*, 8956–8963.

[25] Wang, C.; Sun, W. J.; Wright, G.; Wang, A. Z.; Gu, Z. Inflammation-triggered cancer immunotherapy by programmed delivery of CpG and anti-PD1 antibody. *Adv. Mater.* **2016**, *28*, 8912–8920.

[26] Hu, Q. Y.; Qian, C. G.; Sun, W. J.; Wang, J. Q.; Chen, Z. W.; Bomba, H. N.; Xin, H. L.; Shen, Q. D.; Gu, Z. Engineered nanoplatelets for enhanced treatment of multiple myeloma and thrombus. *Adv. Mater.* **2016**, *28*, 9573–9580.

[27] Sirsi, S. R.; Borden, M. A. State-of-the-art materials for ultrasound-triggered drug delivery. *Adv. Drug. Deliv. Rev.* **2014**, *72*, 3–14.

[28] Di, J.; Price, J.; Gu, X.; Jiang, X. N.; Jing, Y.; Gu, Z. Ultrasound-triggered regulation of blood glucose levels using injectable nano-network. *Adv. Healthc. Mater.* **2014**, *3*, 811–816.

[29] Huebsch, N.; Kearney, C. J.; Zhao, X. H.; Kim, J.; Cezar, C. A.; Suo, Z. G.; Mooney, D. J. Ultrasound-triggered disruption and self-healing of reversibly cross-linked hydrogels for drug delivery and enhanced chemotherapy. *Proc. Natl. Acad. Sci. USA* **2014**, *111*, 9762–9767.

[30] Wang, J. L.; Kaplan, J. A.; Colson, Y. L.; Grinstaff, M. W. Mechanoresponsive materials for drug delivery: Harnessing forces for controlled release. *Adv. Drug. Deliv. Rev.* **2017**, *108*, 68–82.

[31] Thévenot, J.; Oliveira, H.; Sandre, O.; Lecommandoux, S. Magnetic responsive polymer composite materials. *Chem. Soc. Rev.* **2013**, *42*, 7099–7116.

[32] Dai, Q.; Nelson, A. Magnetically-responsive self assembled composites. *Chem. Soc. Rev* **2010**, *39*, *4057–4066*.

[33] Yu, J. C.; Zhang, Y. Q.; Sun, W. J.; Wang, C.; Ranson, D.; Ye, Y. Q.; Weng, Y. Y.; Gu, Z. Internalized compartments encapsulated nanogels for targeted drug delivery. *Nanoscale* **2016**, *8*, 9178–9184.

[34] Lu, Y.; Sun, W. J.; Gu, Z. Stimuli-responsive nanomaterials for therapeutic protein delivery. *J. Control. Release* **2014**, *194*, 1–19.

[35] Hu, Q. Y.; Katti, P. S.; Gu, Z. Enzyme-responsive nanomaterials for controlled drug delivery. *Nanoscale* **2014**, *6*, 12273–12286.

[36] Mayumi, K.; Marcellan, A.; Ducouret, G.; Creton, C.; Narita, T. Stress-strain relationship of highly stretchable dual cross-link gels: Separability of strain and time effect. *ACS Macro Lett.* **2013**, *2*, 1065–1068.

[37] Kampa M.; Nifli, A. P.; Notas G.; Castanas E. Polyphenols and cancer cell growth. In *Reviews of Physiology*, *Biochemistry and Pharmacology*; Amara, S.; Bamberg, E.; Fleischmann, B.; Gudermann, T.; Hebert, S. C.; Jahn, R.; Lederer, W. J.; Lill, R.; Miyajima, A.; Offermanns, S. et al., Eds.; Springer: Berlin, Heidelberg, 2007.

[38] Shukla, M.; Gupta, K.; Rasheed, Z.; Khan, K. A.; Haqqi, T. M. Consumption of hydrolyzable tannins-rich pomegranate extract suppresses inflammation and joint damage in rheumatoid arthritis. *Nutrition* **2008**, *24*, 733–743.

[39] Rasheed, Z.; Anbazhagan, A. N.; Akhtar, N.; Ramamurthy, S.; Voss, F. R.; Haqqi, T. M. Green tea polyphenol epigallocatechin-3-gallate inhibits advanced glycation end product-induced expression of tumor necrosis factor-α and matrix metalloproteinase-13 in human chondrocytes. *Arthritis Res. Ther.* **2009**, *11*, R71.

[40] Yesilyurt, V.; Webber, M. J.; Appel, E. A.; Godwin, C.; Langer, R.; Anderson, D. G. Injectable self-healing glucose-responsive hydrogels with pH-regulated mechanical properties. *Adv. Mater.* **2016**, *28*, 86–91.

[41] Dong, Y. Z.; Wang, W. H.; Veiseh, O.; Appel, E. A.; Xue, K.; Webber, M. J.; Tang, B. C.; Yang, X. W.; Weir, G. C.; Langer, R. et al. Injectable and glucose-responsive hydrogels based on boronic acid–glucose complexation. *Langmuir* **2016**, *32*, 8743–8747.

[42] Bapat, A. P.; Roy, D.; Ray, J. G.; Savin, D. A.; Sumerlin, B. S. Dynamic-covalent macromolecular stars with boronic ester linkages. *J. Am. Chem. Soc.* **2011**, *133*, 19832–19838.

[43] Cromwell, O. R.; Chung, J.; Guan, Z. B. Malleable and self-healing covalent polymer networks through tunable dynamic boronic ester bonds. *J. Am. Chem. Soc.* **2015**, *137*, 6492–6495.

[44] He, L. H.; Fullenkamp, D. E.; Rivera, J. G.; Messersmith, P. B. pH responsive self-healing hydrogels formed by boronate–catechol complexation. *Chem. Commun.* **2011**, *47*, 7497–7499.

[45] Leslie, K. O.; Trahan, S.; Gruden, J. Pulmonary pathology of the rheumatic diseases. *Semin. Resp. Crit. Care* **2007**, *28*, 369–378.